arXiv:1403.4715v1 [cond-mat.supr-con] 19 Mar 2014

Is the anisotropy of the upper critical field of Sr_2RuO_4 consistent with a helical p-wave state?

Jingchuan Zhang and Qiang Gu
Department of Physics, University of Science and Technology Beijing, Beijing 100083, China

Christopher Lörscher and Richard A. Klemm
Department of Physics, University of Central Florida, Orlando, FL 32816-2385 USA

(Dated: February 28, 2022)

We calculate the angular and temperature T dependencies of the upper critical field $H_{c2}(\theta,\phi,T)$ for the C_{4v} point group helical p-wave states, assuming a single uniaxial ellipsoidal Fermi surface, Pauli limiting, and strong spin-orbit coupling that locks the spin-triplet $\boldsymbol{d}$-vectors onto the layers. Good fits to the Sr_2RuO_4 $H_{c2,a}(\theta,T)$ data of Kittaka *et al.* [2009 *Phys. Rev.* B **80**, 174514] are obtained. Helical states with $\boldsymbol{d}(\boldsymbol{k}) = \hat{k}_x\hat{\boldsymbol{x}} - \hat{k}_y\hat{\boldsymbol{y}}$ and $\hat{k}_y\hat{\boldsymbol{x}} + \hat{k}_x\hat{\boldsymbol{y}}$ (or $\hat{k}_x\hat{\boldsymbol{x}} + \hat{k}_y\hat{\boldsymbol{y}}$ and $\hat{k}_y\hat{\boldsymbol{x}} - \hat{k}_x\hat{\boldsymbol{y}}$) produce $H_{c2}(90^\circ,\phi,T)$ that greatly exceed (or do not exhibit) the four-fold azimuthal anisotropy magnitudes observed in Sr_2RuO_4 by Kittaka *et al.* and by Mao *et al.* [2000 *Phys. Rev. Lett.* **84** 991], respectively.

INTRODUCTION

Despite two decades of extensive studies the detailed structure of the superconducting order parameter in Sr_2RuO_4 remains unclear [1–3]. Nuclear magnetic resonance (NMR) and nuclear quadruple resonance (NQR) Knight shift measurements of the electronic spin susceptibility of the O [4, 5] and Ru [6–8] nuclear sites, internal magnetic field measurements by spin-polarized neutron scattering [9, 10] and spin-relaxation measurements by muon spin resonance (μSR) [11] all provided support to a parallel-spin pairing state. The invariance of the spin susceptibility on entering the superconducting state with the magnetic field $\boldsymbol{H}$ both parallel and perpendicular to the RuO_2 layers was argued to be consistent with very weak spin-orbit coupling in Sr_2RuO_4, so that the d-vector representing the orientation of the spin-triplet pairing state would always rotate to be perpendicular to $\boldsymbol{H}$ for $\mu_0 H > 20$ mT [7], where μ_0 is the vacuum magnetic permeability. However, this scenario is in direct conflict with the suppression of the in-plane upper critical field $H_{c2,ab}$ (~ 1.5 T) at low temperatures T [12–14], reminiscent of the strong Pauli pairbreaking limit in spin-singlet pair states [15] or a spin-triplet pair state with the d-vector parallel to the field [16]. Indeed, with the assumption that the d-vector is locked in some direction in the basal plane, the suppression of $H_{c2,ab}$ could possibly be explained by the inclusion of Pauli pairbreaking [17, 18]. The discrepancies in the orientation of the d-vector are even aggravated by the extreme sensitivity of the $H_{c2,ab}$ suppression [13] as well as by the in-plane anisotropy of $H_{c2,ab}(\phi)$ [19, 20] to the precise field alignment. Although introducing a multi-component order parameter seems rather unconvincing that it might apply to all cases [21, 22], it might be relevant to the chiral-nonchiral transition in vortex states [23, 24] or even to the first-order transition to the normal state [14]. Further complicating matters, one set of scanning tunneling microscopy (STM) experiments was consistent with a single nodeless gap on all three Fermi surfaces of Sr_2RuO_4 [25], but in another STM experiment, the tip was placed in a spot with substantial normal regions for $T \ll T_c$ [26], completely disguising any possible superconducting order parameter form. To gain a possibly consistent interpretation to all pieces of experimental evidence, it appears indispensable to introduce a new mechanism to describe the nontrivial interaction between spin-triplet superconductivity and $\boldsymbol{H}$. Beforehand, one could nevertheless assume that the Pauli limit was essential to determine the in-plane $H_{c2,ab}$. In addition, since many examples of anomalous Knight shift results in singlet-spin layered and heavy fermion superconductors have been obtained, a new theory of the Knight shift is sorely needed [27, 28].

The possible spin-triplet p-wave states for Sr_2RuO_4 are limited by the tetragonal crystal structure with two-dimensional square lattice point group symmetry C_{4v} to the six degenerate states with the d-vectors $\hat{k}_x\hat{\boldsymbol{x}} \pm \hat{k}_y\hat{\boldsymbol{y}}$, $\hat{k}_y\hat{\boldsymbol{x}} \pm \hat{k}_x\hat{\boldsymbol{y}}$ and $(\hat{k}_x \pm i\hat{k}_y)\hat{\boldsymbol{z}}$ [30, 31]. The two chiral states $\boldsymbol{d} = (\hat{k}_x \pm i\hat{k}_y)\hat{\boldsymbol{z}}$ with $\boldsymbol{d} \parallel \hat{\boldsymbol{c}}$ are believed to be stabilized near $\boldsymbol{H} = 0$ [1, 3], while with $H \sim H_{c2,ab}$, only the four helical states with d-vectors lying in the basal plane could be consistent with the in-plane $H_{c2,ab}$ measurements [13] by including the effects of Pauli limiting [18]. Contrary to the the assumption of very weak spin-orbit coupling, allowing the d-vector to rotate to a direction perpendicular to $\boldsymbol{H}$, that was argued to explain the Knight shift observations for both $\boldsymbol{H}||\hat{\boldsymbol{c}}$ and $\boldsymbol{H} \perp \hat{\boldsymbol{c}}$, sufficiently strong spin-orbit coupling should be assumed to allow for Zeeman energy splitting in spin-triplet pairing states[29]. In this case, the degeneracy in the four helical states is lifted [2], since each state responds differently to $\boldsymbol{H}$, as illustrated in figure 1, two of them manifesting themselves by showing intrinsic four-fold in-plane anisotropies of $H_{c2,ab}(\phi)$ — a novel scenario other

than earlier postulations of a multi-component order parameter [21] or the possible misalignment of two domains in the sample [13]. In this paper, we will calculate the full angular and T dependencies of $H_{c2}(\theta,\phi,T)$ for the four helical states to try to set further restrictions on the possible pairing symmetries in Sr_2RuO_4.

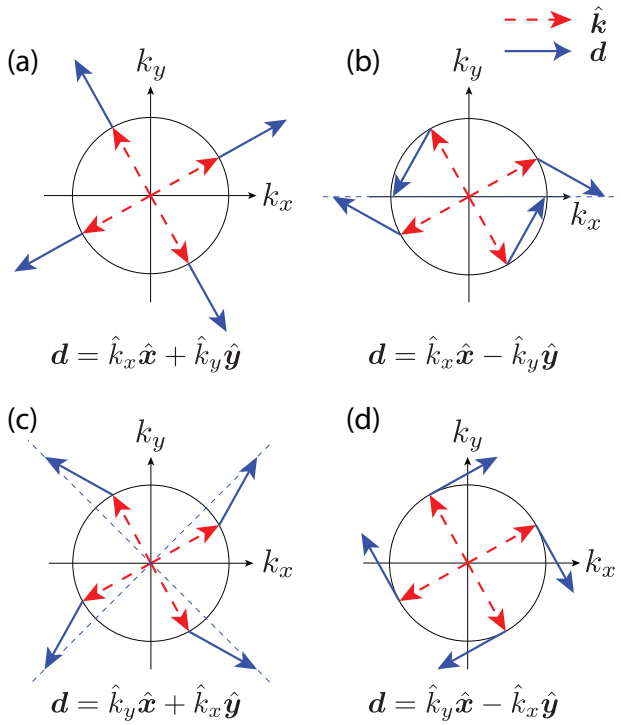


FIG. 1. Illustration of the d-vectors for the helical states. In terms of $H_{c2,ab}(\phi)$, helical states shown in (a) and (d) are isotropic, while those in (b) and (c) exhibit four-fold in-plane anisotropies due to the Pauli paramagnetic effect and strong spin-orbit coupling.

MODEL

The Fermi surface of Sr_2RuO_4 consists of three sheets: a quasi-two-dimensional γ band, and a pair of quasi-one-dimensional (α, β) bands [32]. Although still under debate [33–35], the cylindrical γ band is widely considered to be the primary source of p-wave pairing [3, 36]. The small c-axis dispersion in this nearly cylindrical γ Fermi surface can be incorporated by treating it as an elongated uniaxial ellipsoid, characterized by the effective mass anisotropy of the quasi-particles $m_c \gg m_a = m_b = m_{ab}$. The primary pair-breaking effects established in superconductivity fall into two categories: 1. the orbital effect arising from the competition between the coherence of two quasi-particles in a Cooper pair and their individual orbital motions in a magnetic field, i.e., the Landau levels governed by the effective vector potential $\boldsymbol{A}$ [37]; 2. the paramagnetic effect due to the Zeeman energy gained from the interactions between their spins and the field [15]. Highly anisotropic Zeeman interactions are expected in the layered compound Sr_2RuO_4, described here by an effective diagonal g-tensor $g = \mathrm{diag}(g_a, g_b, g_c)$ with $g_c \neq g_a = g_b = g_{ab}$ as in $-\mu_B \boldsymbol{S}\cdot g\cdot \overline{m}_{1/2}\cdot \boldsymbol{B}$, where μ_B is the Bohr magneton, $\boldsymbol{S}$ is the electron spin, $\overline{m}_{1/2} = \mathrm{diag}(\overline{m}_a^{1/2}, \overline{m}_b^{1/2}, \overline{m}_c^{1/2})$ is the diagonal tensor of the square roots of the relative effective masses $\overline{m}_\mu = m_\mu/m$ ($\mu = a, b, c$) with geometric mean effective mass $m = (m_a m_b m_c)^{1/3}$, and the magnetic induction $\boldsymbol{B} = \mu_0\boldsymbol{H} + \boldsymbol{M} = \nabla\times\boldsymbol{A}$, where $\boldsymbol{M}$ is the magnetization proportional to $\boldsymbol{H}$ for the non-ferromagnetic superconductor Sr_2RuO_4 [11]. If the d-vector is along the c axis, neither the chiral Anderson-Brinkman-Morel (ABM) state $\Delta_0(\hat{k}_x + i\hat{k}_y)\hat{\boldsymbol{z}}$ [38, 39] nor the Scharnberg-Klemm (SK) state $[\Delta_{0+}(\hat{k}_x + \hat{k}_y) + \Delta_{0-}(\hat{k}_x - i\hat{k}_y)]\hat{\boldsymbol{z}}$ [24, 40], nor generalizations of them obtained by setting $\hat{k}_x \to \sin(k_x a)$ and $\hat{k}_y \to \sin(k_y a)$ [26], could fit the in-plane $H_{c2,ab}$ measurements; for comparison, even the conventional s-wave state without Pauli limiting has $H_{c2}(T)$ well above the experimental data of Kittaka *et al.* for $\boldsymbol{H}||\hat{\boldsymbol{a}}$ (figure 2). Instead, the helical states have a chance for Pauli limiting to play the crucial role in suppressing $H_{c2,ab}(T)$, as long as $\boldsymbol{H}$ cannot cause the d-vectors to rotate.

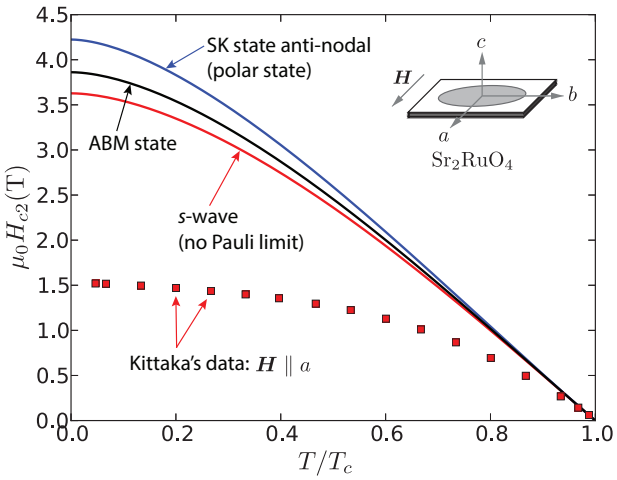


FIG. 2. Fits of the chiral ABM, SK and s-wave (without Pauli limiting) states to the in-plane $H_{c2,a}(T)$ measurements of Sr_2RuO_4 [13]. The in-plane $H_{c2,ab}(T)$ is strongly suppressed at low temperatures from than predicted from the orbital pairbreaking in these states. Note that in the anti-nodal direction, $H_{c2,ab}(T)$ of the chiral SK state has a first-order transition to that of the nonchiral polar state $\boldsymbol{d} = \Delta_0 k_x\hat{\boldsymbol{z}}$ [24].

Hence we model Sr_2RuO_4 as a clean homogeneous weak-coupling type-II superconductor. Since close to H_{c2}, $\Delta(\boldsymbol{R}) = \sum_{n=0}^{\infty} a_n\,|n(\boldsymbol{R})\rangle$ for the vortex lattice in the mixed state, is constructed from the harmonic oscillator states $|n\rangle$, and is vanishingly small, the Gor'kov equations for p-wave superconductors with a single ellipsoidal Fermi surface can be linearized and transformed

to yield [40, 41, 44]

$$\Delta(\boldsymbol{R}) = 2\pi T N(0) V_0 \sum_{\omega_n} \int \frac{\mathrm{d}\Omega_{\boldsymbol{k}'}}{4\pi} \int_0^\infty \mathrm{d}\xi \exp\left[-2|\omega_n|\xi\right] \times \exp\Big[-i\,\mathrm{sgn}\omega_n \xi \boldsymbol{v}_F(\hat{\boldsymbol{k}}') \cdot \Big(\alpha\nabla_{\boldsymbol{R}}/i + 2e\boldsymbol{A}\Big)\Big]\Delta(\boldsymbol{R}) \times \Big(\big|\boldsymbol{d}(\hat{\boldsymbol{k}}')\big|^2 + [\cos(\alpha g_{\rm eff}\mu_B B\xi) - 1]\big|d_z(\hat{\boldsymbol{k}}')\big|^2\Big), \quad (1)$$

where $N(0)$ is the density of states per spin at the Fermi level, V_0 is the pairing amplitude, ω_n are the fermion Matsubara frequencies, $\boldsymbol{v}_F = \boldsymbol{k}_F/m$ is the effective Fermi velocity, $\alpha = (\overline{m}_{ab}\sin^2\theta + \overline{m}_c\cos^2\theta)^{1/2}$ characterizes the geometric anisotropy of the Fermi surface, $g_{\rm eff} = \left[g_c^2\cos^2\theta' + g_{ab}^2\sin^2\theta'\right]^{1/2}$ is the effective g-factor experienced by the spins with $\cos\theta' = \sqrt{\overline{m}_c}\cos\theta/\alpha$, e is the electronic charge and the convention $\hbar = c = k_B = 1$ is adopted. We note that the Klemm-Clem (KC) transformations have been performed so that the $\hat{\boldsymbol{z}}'$ direction in (1) is always along $\boldsymbol{B}'$ [42–44].

All of the helical states in figure 1 are degenerate in terms of the KC transformed $\big|\boldsymbol{d}(\hat{\boldsymbol{k}}')\big|^2 = (\hat{k}'_x\cos\theta' + \hat{k}'_z\sin\theta')^2 + \hat{k}'^2_y$. However, the z-components $\big|d_z(\hat{\boldsymbol{k}}')\big|^2 = |\hat{\boldsymbol{B}}'\cdot\boldsymbol{d}(\hat{\boldsymbol{k}}')|^2$, which contribute to the Zeeman energy, are distinct for each of the four helical states. For the helical state $\boldsymbol{d} = \hat{k}_x\hat{\boldsymbol{x}} - \hat{k}_y\hat{\boldsymbol{y}}$ in figure 1(b), the KC transformed

$$\big|d_z(\hat{\boldsymbol{k}}')\big|^2 = \big(g_{ab}/g_{\rm eff}\big)^2\sin^2\theta'\big[(\hat{k}'_x\cos\theta' + \hat{k}'_z\sin\theta')\cos 2\phi - \hat{k}'_y\sin 2\phi\big]^2, \quad (2)$$

is anisotropic in the basal plane[42, 43], where $\phi' = \phi$ for $m_a = m_b$, and for consistency we set $\hat{k}'_y \to \hat{k}'_x$ and $\hat{k}'_x \to -\hat{k}'_y$. $\big|d_z(\hat{\boldsymbol{k}}')\big|^2$ in state (c) is obtained from that of helical state (b) in (2) by letting $\phi \to \phi - \pi/4$, while $\big|d_z(\hat{\boldsymbol{k}}')\big|^2$ for the helical states (a) and (d) are respectively obtained by setting $\phi = 0$ and $\phi = \pi/4$ in (2). These latter two helical states are therefore isotropic in the basal plane. Accordingly, the helical state (b) with $\boldsymbol{d} = \hat{k}_x\hat{\boldsymbol{x}} - \hat{k}_y\hat{\boldsymbol{y}}$ can be used to present the formulation.

We introduce the dimensionless quantities $t = T/T_c(0)$, $b_{c2} = B_{c2}/B_0$ and for the g-tensor (via its elements) $\bar{g} = g/g_0$, where $T_c(0) = (2e^C\omega_c/\pi)e^{-1/N(0)V_0}$ is the superconducting transition temperature in zero field, $C = 0.577$ is the Euler constant, ω_c is the energy cutoff from the BCS theory, $B_0 = [2\pi T_c(0)]^2/2ev_F^2$ and $g_0 = 2\pi T_c(0)/\mu_B B_0$. Equation (1) can be expanded as [40]

$$\big[-\ln t + \alpha_n^{(p)} + \alpha_n^{(a)}\big]a_n + \beta_{n-2}^{(+)}a_{n-2} + \beta_n^{(-)}a_{n+2} = 0. \quad (3)$$

The upper critical field b_{c2} is embedded in the coefficients

$$\alpha_n^{(p)} = \int_0^\infty \mathrm{d}\psi \frac{\sinh^2\psi}{\cosh^3\psi}\int_0^\infty \mathrm{d}\rho \frac{t\sqrt{2/\alpha b_{c2}}}{\sinh\big(t\sqrt{2/\alpha b_{c2}}\rho\cosh\psi\big)} \times\Big[e^{-\frac{1}{2}\rho^2}L_n^{(0)}(\rho^2)F^{(p)} - \sin^2\theta'\Big], \quad (4)$$

$$\alpha_n^{(a)} = \int_0^\infty \mathrm{d}\psi \frac{1}{2\cosh^3\psi}\int_0^\infty \mathrm{d}\rho \frac{t\sqrt{2/\alpha b_{c2}}}{\sinh\big(t\sqrt{2/\alpha b_{c2}}\rho\cosh\psi\big)} \times\Big[e^{-\frac{1}{2}\rho^2}L_n^{(0)}(\rho^2)F^{(a)} - (1+\cos^2\theta')\Big], \quad (5)$$

$$\beta_n^{(\pm)} = \int_0^\infty \mathrm{d}\psi \frac{1}{4\cosh^3\psi}\int_0^\infty \mathrm{d}\rho \frac{t\sqrt{2/\alpha b_{c2}}}{\sinh\big(t\sqrt{2/\alpha b_{c2}}\rho\cosh\psi\big)} \times e^{-\frac{1}{2}\rho^2}\frac{-\rho^2}{\sqrt{(n+2)(n+1)}}L_n^{(2)}(\rho^2) \times\Big[-\sin^2\theta' + G(\cos^2\theta'\cos^2 2\phi - \sin^2 2\phi) \pm iG\cos\theta'\sin 4\phi\Big], \quad (6)$$

where the $L_n^{(m)}$ are the associated Laguerre polynomials, and

$$F^{(p)} = \sin^2\theta' + G\sin^2\theta'\cos^2 2\phi, \quad (7)$$

$$F^{(a)} = 1 + \cos^2\theta' + G(\cos^2\theta'\cos^2 2\phi + \sin^2 2\phi) \quad (8)$$

with $G = \big[\cos\big(\bar{g}_{\rm eff}\sqrt{\alpha b_{c2}/2}\big) - 1\big]\big(\bar{g}_{ab}/\bar{g}_{\rm eff}\big)^2\sin^2\theta'$. The solution to (3) constitutes the determinant of the (infinite order) tridiagonal matrix constructed from the coefficients of a_n ($n = 0, 2, \dots$), which can be solved numerically for arbitrary t. To calculate $B_{c2} = \mu_0 H_{c2}$ for non-magnetic superconductors, usually the first 3 or 4 orders produce sufficiently accurate results to show all of the essential features.

RESULTS

Figure 3 shows our fits to the angular dependent $H_{c2,a}(\theta, T)$ measurements of Kittaka *et al.* on a sample of Sr_2RuO_4 ($T_c(0) = 1.503$ K) [13] using helical state (b) with $\boldsymbol{d} = \hat{k}_x\hat{\boldsymbol{x}} - \hat{k}_y\hat{\boldsymbol{y}}$. The appropriateness of an elongated uniaxial ellipsoidal Fermi surface for the γ band is verified by the huge effective mass anisotropy $m_c/m_{ab} = 1067$ estimated from the slopes of $H_{c2,a}(T)$ at $T_c(0)$ in the [100] and [001] crystal directions where Pauli limiting effects are neglibible. Down to low t, a suitable choice of the effective g-factor will further suppress the H_{c2} curves, especially for those with $\theta < 5^\circ$ (c.f. figure 2). Although the $H_{c2,a}(T, \theta > 5^\circ)$ data appear to follow the anisotropic effective mass model [13, 24, 44], one should nevertheless take into consideration the intrinsic anisotropy of $H_{c2}(\theta)$ raising from the point nodal structures of the helical states ($[H_{c2,ab}/H_{c2,c}]_{T\to T_c(0)} = \sqrt{2}$ for an isotropic Fermi surface) [24]. For an overall best fit, the effective g-tensor was evaluated to have the diagonal elements

$\bar{g}_c = 0.2$ and $\bar{g}_{ab} = 1.9$. Obviously, the small-valued $\bar{g}_c$ doesn't contribute to $H_{c2,c}$ since $\boldsymbol{d} \perp \hat{\boldsymbol{c}}$ for the helical states, but it plays a role in determining $H_{c2}(\theta)$ for $(0° < \theta < 90°)$.

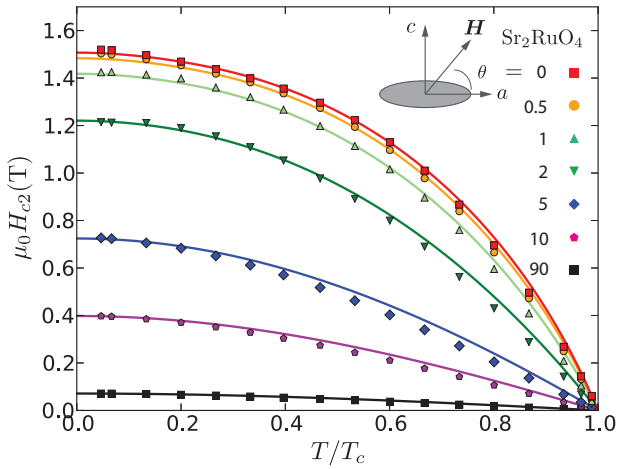


FIG. 3. Fits to the angular dependent $H_{c2,a}(\theta, T)$ measurements of Sr_2RuO_4 sample [13] using helical state (b) with $\boldsymbol{d} = \hat{k}_x\hat{\boldsymbol{x}} - \hat{k}_y\hat{\boldsymbol{y}}$ with $\bar{g}_{ab} = 1.9$, $\bar{g}_c = 0.2$.

We remark that all the helical states listed in figure 1 could equally well fit the data shown in figure 3, as the differences in their H_{c2} values only appear in their in-plane (ϕ) anisotropies. As seen from (1), in the absence of Pauli limiting, $H_{c2,ab}(\phi)$ for the helical states are isotropic in the basal plane. However, with the fitting parameter $\bar{g}_{ab} = 1.9$, the $H_{c2,ab}(\phi)$ at 0.13 K for the helical states (b) and (c) in figure 1 exhibit four-fold in-plane azimuthal anisotropies with a relative amplitude as large as 30% (figure 4(a)) and a phase shift of $\pi/4$ between them, while those for states (a) and (d) remain isotropic in the ab plane. The observed in-plane anisotropy of $H_{c2,ab}(\phi)$ is at most 3% and disappears either above 0.8 K or with a field misalignment of less than 1° [13, 19]. The calculated anisotropy for helical state (b) with $\boldsymbol{d} = \hat{k}_x\hat{\boldsymbol{x}} - \hat{k}_y\hat{\boldsymbol{y}}$ state persists for $T > T_c/2$ and for field misalignments greater than 2° (figure 4(b)). Thus, this parallel-spin p-wave state can explain the strong Pauli limiting for $\boldsymbol{B} \perp \hat{\boldsymbol{c}}$, but the details are not in precise agreement with the experimental observations [13, 19].

DISCUSSION

A multi-component order parameter proposed to interpret the in-plane $H_{c2,ab}(\phi)$ anisotropy in reference [19] turns out to have a similar problem of a large magnitude of the in-plane anisotropy [21]. There could also be two slightly misaligned crystals in the same sample [13], and the smaller region of the hysteretic magnetization data below 0.8 K in the more recent data of Yonezawa *et al.* than in the older Mao *et al.* and

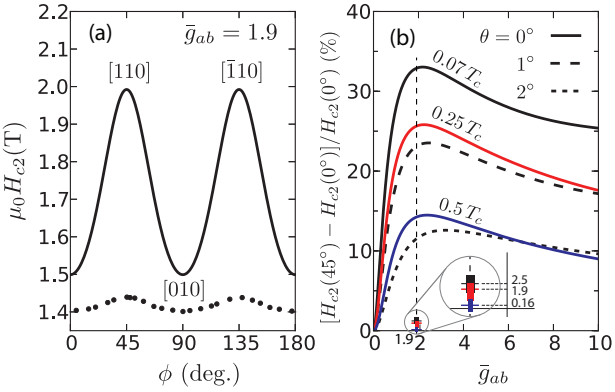


FIG. 4. In-plane $H_{c2,ab}(\phi)$ anisotropy of helical state (b) with $\boldsymbol{d} = k_x\hat{\boldsymbol{x}} - k_y\hat{\boldsymbol{y}}$. (a) $H_{c2,ab}(\phi)$ with an effective g-factor $\bar{g}_{ab} = 1.9$ at 0.13 K . The amplitude of the predicted anisotropy (solid) is an order of magnitude larger than that (dotted curve) observed in Sr_2RuO_4 by Mao *et al.*[19]. (b) Effects of g_{eff} to the relative magnitudes of the in-plane anisotropy at various temperatures and field misalignments. Anisotropies comparable to the experiments only occur with small $\overline{g}_{ab}$ values. The symbols at the bottom represent the data of Kittaka *et al.*[13].

Deguchi *et al.* data are consistent with this scenario[12–14, 19]. Others think that this first-order transition below 0.8 K is more intrinsically due to a Fulde-Farrell-Larkin-Ovchinnikov state, entered below $0.55T_c$ (close to 0.8 K in Sr_2RuO_4) [45]. Based on the present calculations, if the Pauli pair-breaking effect is demanded as the source for the suppression on $H_{c2,ab}$, helical state (b) with $\boldsymbol{d} = \hat{k}_x\hat{\boldsymbol{x}} - \hat{k}_y\hat{\boldsymbol{y}}$ has the same four-fold anisotropy with the same phase as in the experiments. Helical state (c) with $\boldsymbol{d} = \hat{k}_y\hat{\boldsymbol{x}} + \hat{k}_x\hat{\boldsymbol{y}}$ has the four-fold anisotropy differing in phase by $\pi/4$. However, both of these azimuthal anisotropies are much stronger than that observed in experiment. However, the other helical (a) and (d) p-wave states with $\boldsymbol{d} = \hat{k}_x\hat{\boldsymbol{x}} + \hat{k}_y\hat{\boldsymbol{y}}$ and $\hat{k}_y\hat{\boldsymbol{x}} - \hat{k}_x\hat{\boldsymbol{y}}$ are predicted to have no azimuthal anisotropies at all. Including ab-planar anisotropy on the γ Fermi surface could lead to a small azimuthal anisotropy of $H_{c2}(90°, \phi, T)$, but normally Fermi surface anisotropy is largest near to T_c. Thus, a single purported triplet-spin order parameter for Sr_2RuO_4 is still elusive. We note, however, that there are many examples in which the Knight shift observations have been misleading and/or are also in apparent conflict with the upper critical field results [28, 46], strongly suggesting that a new theory of the Knight shift might lead to a possible resolution of the symmetry of the order parameter in Sr_2RuO_4[27, 28].

In summary, we studied the four helical p-wave states potentially realized in Sr_2RuO_4 at H_{c2} by fitting the angular dependent $H_{c2,a}(\theta, \phi, T)$ measurements, taking the Pauli paramagnetic effects into account by imposing strong spin-orbit coupling effects as the origin of the $H_{c2,ab}$ suppression. In the ranges of the fitting parame-

ters, one of the four helical states was predicted to have in-plane $H_{c2}(90°, \phi, T)$ four-fold azimuthal anisotropy with the same phase as observed, but both that azimuthal anisotropy and that from the (c) helical state with the anisotropy shifted by $\pi/4$ in phase, had amplitudes that were predicted to be much stronger than that observed in Sr_2RuO_4. The $H_{c2}(90°, \phi, T)$ behaviors of the two other helical p-wave states were predicted to be completely independent of ϕ, as long as in-plane Fermi surface anisotropy could be safely ignored. Other attempts to fit an order parameter such as $\Delta_0[\sin(k_x a) + i \sin(k_y a)]$ with the low-T specific heat $C_V \sim T^2$ dependence failed to confront the very strong Pauli limiting of $H_{c2}(90°, \phi, T)$[26]. Thus, the thermodynamic zero-field specific heat measurements appear to be in direct conflict with the field-dependent thermodynamic specific heat and magnetization measurements of the upper critical field[12–14, 19]. Further calculations to try to fit the excellent scanning tunneling microscopy results of Suderow *et al.* with a p-wave order parameter are also needed[25]. A point node in a helical p-wave order parameter might smear the sharp density of states walls they observed, but an accurate calculation is needed to quantify this possible disagreement.

ACKNOWLEDGMENTS

We thank S. Kittaka for supplying us with his published $H_{c2}(\theta, \phi, T)$ data. This work is partially supported by the National Natural Science Foundation of China (Grant No. 11274039) and the Specialized Research Fund for the Doctoral Program of Higher Education (No. 20100006110021). QG acknowledges helpful discussions with Prof. John Chalker and is grateful for the support from the China Scholarship Council and the hospitality of the Rudolf Peierls Centre for Theoretical Physics, University of Oxford.

REFERENCES

[1] Mackenzie A P 2003 *Rev. Mod. Phys.* **75** 657–712
[2] Sigrist M 2005 *Prog. Theor. Phys. Supplement* **160** 1–14
[3] Maeno Y, Kittaka S, Nomura T, Yonezawa S and Ishida K 2012 *J. Phys. Soc. Jpn.* **81** 011009
[4] Ishida K, Mukuda H, Kitaoka Y, Asayama K, Mao Z Q, Mori Y and Maeno Y 1998 *Nature* **396** 658–660
[5] Mukuda H, Ishida K, Kitaoka Y, Mao Z, Mori Y and Maeno Y 1999 *J Low Temp. Phys.* **117** 1587–1591
[6] Ishida K, Mukuda H, Kitaoka Y, Mao Z, Fukazawa H and Maeno Y 2001 *Phys. Rev.* B **63** 060507
[7] Murakawa H, Ishida K, Kitagawa K, Mao Z and Maeno Y 2004 *Phys. Rev. Lett.* **93** 167004
[8] Murakawa H, Ishida K, Kitagawa K, Ikeda H, Mao Z Q and Maeno Y 2007 *J. Phys. Soc. Jpn.* **76** 024716
[9] Riseman T M, Kealey P G, Forgan E M, Mackenzie A P, Galvin L M, Tyler A W, Lee S L, Ager C, Paul D M, Aegerter C M, Cubitt R, Mao Z Q, Akima T and Maeno Y 1998 *Nature* **396** 242–245
[10] Duffy J, Hayden S, Maeno Y, Mao Z, Kulda J and McIntyre G 2000 *Phys. Rev. Lett.* **85** 5412–5415
[11] Luke G M, Fudamoto Y, Kojima K M, Larkin M I, Merrin J, Nachumi B, Uemura Y J, Maeno Y, Mao Z Q, Mori Y, Nakamura H and Sigrist M 1998 *Nature* **394** 558–561
[12] Deguchi K, A Tanatar M, Mao Z, Ishiguro T and Maeno Y 2002 *J. Phys. Soc. Jpn.* **71** 2839–2842
[13] Kittaka S, Nakamura T, Aono Y, Yonezawa S, Ishida K and Maeno Y 2009 *Phys. Rev.* B **80** 174514
[14] Yonezawa S, Kajikawa T and Maeno Y 2013 *Phys. Rev. Lett.* **110** 077003
[15] Clogston A M 1962 *Phys. Rev. Lett.* **9** 266–267
[16] Leggett A J 1975 *Rev. Mod. Phys.* **47** 331–414
[17] Machida K and Ichioka M 2008 *Phys. Rev.* B **77** 184515
[18] Choi C H 2010 *J. Korean Phys. Soc.* **56** 933
[19] Mao Z Q, Maeno Y, NishiZaki S, Akima T and Ishiguro T 2000 *Phys. Rev. Lett.* **84** 991–994
[20] Deguchi K, Mao Z Q, Yaguchi H and Maeno Y 2004 *Phys. Rev. Lett.* **92** 047002
[21] Agterberg D 2001 *Phys. Rev.* B **64** 052502
[22] Mineev V P 2008 *Phys. Rev.* B **77** 064519
[23] Ishihara M, Amano Y, Ichioka M and Machida K 2013 *Phys. Rev.* B **87** 224509
[24] Zhang J, Lörscher C, Gu Q and Klemm R A 2014 *arXiv* (*Preprint* 1401.2178v1)
[25] Suderow H, Crepo V, Guillamon I, Viera S, Servant F, Lejay P, Brison J P and Flouquet J 2009 *New J. Phys.* **11** 093004
[26] Firmo I A, Lederer S, Lupien C, Mackenzie A P, Davis J C and Kivelson S A 2013 *Phys. Rev.* B **88** 134521
[27] Pavarini E and Mazin I 2006 *Phys. Rev.* B **74** 035115; *ibid* (2007) **76** 079901(E)
[28] Hall B E and Klemm R A 2014 (unpublished)
[29] Rozbicki E J, Annett J F, Souquet J R and Mackenzie A P 2011 *J. Phys. Condens. Matter* **23** 094201
[30] Sigrist M and Ueda K 1991 *Rev. Mod. Phys.* **63** 239–311
[31] Rice T M and Sigrist M 1999 *J. Phys.: Condens. Matter* **7** L643–L648
[32] Bergemann C, Julian S, Mackenzie A P, NishiZaki S and Maeno Y 2000 *Phys. Rev. Lett.* **84** 2662–2665
[33] Raghu S, Kapitulnik A and Kivelson S A 2010 *Phys. Rev. Lett.* **105** 136401
[34] Annett J, Litak G, Györffy B and Wysokiński K 2002 *Phys. Rev.* B **66** 134514
[35] Zhitomirsky M and Rice T 2001 *Phys. Rev. Lett.* **87** 057001
[36] Huo J W, Rice T and Zhang F C 2013 *Phys. Rev. Lett.* **110** 167003
[37] Helfand E and Werthamer N R 1966 *Phys. Rev.* **147** 288–294
[38] Anderson P W and Morel P 1961 *Phys. Rev.* **123** 1911–1934
[39] Anderson P and Brinkman W 1973 *Phys. Rev. Lett.* **30** 1108–1111
[40] Klemm R A and Scharnberg K 1980 *Phys. Rev.* B **22** 5233–5244
[41] Choi C and Sauls J 1993 *Phys. Rev.* B **48** 13684–13690
[42] Klemm R A and Clem J R 1980 *Phys. Rev.* B **21** 1868

[43] Klemm R A 2012 *Layered Superconductors:* (Oxford University Press, Oxford UK and New York NY)
[44] Lörscher C, Zhang J, Gu Q and Klemm R A 2013 *Phys. Rev.* B **88** 024504
[45] Matsuda Y and Shimahara H 2007 *J. Phys. Soc. Jpn.* **76** 051005
[46] Noer R J and Knight W D 1964 *Rev. Mod. Phys.* **36** 177–184